

# A “Double-Multi” Model for Electromigration of Lithiums and Chlorides in ASR Affected Concrete

Q.F. Liu, L.X. Mao and Z. Hu

State Key Laboratory of Ocean Engineering, Shanghai Jiao Tong University, China; Collaborative Innovation Center for Advanced Ship and Deep-Sea Exploration (CISSE), Shanghai, China

J. Xia

Institute of Structural Engineering, Zhejiang University, Hangzhou, China

G.L. Feng and L.Y. Li

School of Marine Science and Engineering, University of Plymouth, UK

## ABSTRACT

*Existing reinforced concrete structures experience severe durability degradation when subjected to alkali-silica reaction (ASR) and chloride attack. A special electrochemical rehabilitation treatment, containing lithium compound anolyte, has been developed to drive lithium ions into concrete as well as remove chlorides simultaneously, for mitigating both the ASR-induced cracks and the chloride-induced corrosion. Good performance of introduced lithiums in controlling ASR-induced expansion has already been proved. Unfortunately, the migration mechanism of lithium in concrete under an external electric field is seldom investigated in existing literature. In this study, with help of the “double-multi” model, the efficiency of impregnation of lithium ions and simultaneously the removal of chloride ions through a specific electrochemical treatment are numerically evaluated, which results into the distribution profiles of all typical ionic species. The heterogeneous concrete model examines the aggregate effect, especially on the interaction with lithiums which are supposed to mitigate ASR. The ionic interaction between different species and the electrochemical reaction at electrodes are also considered. Through a relative thorough modelling of multi-phase and multi-species, a systemic parametric analysis based on a series of significant factors during electrochemical treatment (e.g., current density, treatment time, temperature, cathode position and concentration of lithium solution) reveals some important tendencies of ionic electromigration in concrete, which are supposed to guide the field application.*

**Keywords:** Alkali-Silica Reaction; Electromigration; Lithium; Electrochemical Rehabilitation; Chloride; ionic transport

## 1.0 INTRODUCTION

Existing reinforced concrete structures experience severe durability degradation when subjected to chloride-induced corrosion and alkali-silica reaction (ASR). The former is due to the destruction of passive film surrounding a steel-rebar when adjacent chlorides reach a threshold concentration (Bazant, 1979). The latter is a chemical reaction between reactive siliceous compounds in aggregates and alkali ions in pore solution, producing a hygroscopic gel, which absorbs water from mortar and swells inducing cracks in the concrete (Powers and Steinour, 1955, Rajabipour *et al.*, 2015). As a result, the ASR affected concrete becomes more vulnerable to chloride attack and making the corrosion of rebar easier. Worse still, the risk of ASR will also increase when treating the chloride-induced corrosion of reinforcement,

especially during the process of electrochemical rehabilitation.

Electrochemical rehabilitation techniques originally developed for treating reinforced concrete structures about to suffer or already suffered from chloride attack (Li and Page, 2000, Liu and Shi, 2012, Martinez *et al.*, 2015) has been proposed to drive lithium ions into concrete to avoid ASR (Page and Yu, 1995, Ueda *et al.*, 2013). During this migration process, not only the lithium ions be impregnated into concrete to anti-ASR but also chloride ions will be removed out to mitigate the chloride-induced corrosion of reinforcing steel. This combined treatment of ELM and ECR (i.e., electrochemical lithium migration and electrochemical chloride removal) involves setting an auxiliary anode surrounded by a lithium-based electrolyte solution on the surface of the concrete and applying a direct

current (DC) density between the anode and the embedded rebar acting as a cathode.

There have been a set number of numerical studies on ionic transport in concrete materials, however, very limited works have been paid on the interaction of different factors on the transport of each individual ionic species. The accurate electro-chemical-physical mechanism of ELM & ECR is not fully understood. In this study, with help of the “double-multi” model (Liu *et al.*, 2012, Liu *et al.*, 2014, Liu *et al.*, 2015b, Geng *et al.*, 2016, Liu *et al.*, 2015a, Liu *et al.*, 2017, Feng *et al.*, 2016, Hu *et al.*, 2018, Liu *et al.*, 2018), the efficiency of impregnation of lithium ions and simultaneously the removal of chloride ions through a specific electrochemical treatment are numerically evaluated, which results into the distribution profiles of all typical ionic species. The heterogeneous concrete model examines the aggregate effect, especially on the interaction with lithiums which are supposed to mitigate ASR. The ionic interaction between different species and the electrochemical reaction at electrodes are also considered. Through a relative thorough modelling of multi-phase and multi-species, a systemic parametric analysis based on a series of significant factors during electrochemical treatment (e.g., current density, treatment time, temperature, cathode position and concentration of lithium solution) reveals some important tendencies of ionic electromigration in concrete, which are supposed to guide the field application.

## 2.0 MULTI-COMPONENT IONIC TRANSPORT IN ELECTROLYTES

The pore solution in concrete involves many ionic species including hydroxyl, sulphate, sodium, potassium, calcium etc., among which the hydroxyl has the highest concentration, followed by the potassium and sodium. The transport of ions in a saturated concrete is mainly by two driving forces, known as the diffusion and migration. The former is due to the concentration gradient of the species itself; the latter is due to the electrostatic potential generated by an externally applied electric field and/or the internal charge imbalance between different species in the solution. The charge imbalance is caused by opposite-direction movement of cations and anions as well as different travel speeds of ions. The exact effect of charge imbalance on the transport of ions in concrete is dependent on the external electric field applied and the difference of diffusion coefficients between ionic species. In general, the effect of charge imbalance on the ionic transport increases with the external electric field and the difference of diffusion coefficients between ionic species. Mathematically, the flux of an ionic species in a multi-component electrolyte solution can be expressed in terms of Nernst-Planck equation as follows,

$$\mathbf{J}_k = -D_k \nabla C_k - D_k C_k \frac{z_k F}{RT} \nabla \Phi \quad (1)$$

where  $J_k$  is the flux,  $C_k$  is the concentration,  $D_k$  is the diffusion coefficient,  $z_k$  is the charge number,  $F = 9.648 \times 10^{-4} \text{ Cmol}^{-1}$  is the Faraday constant,  $R = 8.314 \text{ J mol}^{-1}\text{K}^{-1}$  is the ideal gas constant,  $T = 298 \text{ K}$  is the absolute temperature,  $\Phi$  is the electrostatic potential, and the subscript  $k$  represents the  $k$ -th ionic species. Eq. (2) is required for each ionic species involved in the solution owing to the mass conservation in unit volume of electrolyte solution,

$$\frac{\partial C_k}{\partial t} = -\nabla \cdot \mathbf{J}_k \quad (2)$$

where  $t$  is the time. Substituting Eq. (1) into (2), it yields,

$$\frac{\partial C_k}{\partial t} = \nabla(D_k \nabla C_k) + \nabla \left[ \left( \frac{z_k D_k F}{RT} \right) C_k \nabla \Phi \right] \quad (3)$$

Note that if the electrostatic potential,  $\Phi$ , in Eq. (3) is purely determined in terms of the externally applied electric field without taking into account the internal charge imbalance between ionic species, that is  $\nabla^2 \Phi = 0$ , then the concentration of each ionic species can be calculated independently by using Eq. (3). Otherwise, the electrostatic potential has to be determined using Poisson’s equation as follows,

$$\nabla^2 \Phi = -\frac{F}{\epsilon_0 \epsilon_r} \sum_{k=1}^N z_k C_k \quad (4)$$

where  $\epsilon_0 = 8.854 \times 10^{-12} \text{ CV}^{-1}\text{m}^{-1}$  is the permittivity of a vacuum,  $\epsilon_r = 78.3$  is the relative permittivity of water at temperature of 298 K, and  $N$  is the total number of species involved in the solution. The use of Poisson’s equation creates two difficulties. One is the coupling of Eq. (3) between different ionic species, since  $\Phi$  is now dependent on not only the boundary conditions governed by the externally applied electric field, but also the concentrations of all ionic species involved in the solution. The other is the nonlinearity and numerical difficulty which involves calculations of large and small numbers that need be handled carefully. Nevertheless, Eqs. (3) and (4) plus initial and boundary conditions can be used to determine the electrostatic potential,  $\Phi$ , and the concentrations of individual ionic species,  $C_k$  ( $k = 1, 2, \dots, N$ ), at any point and any time in the solution domain.

## 3.0 IONIC TRANSPORT IN THE MEDIUM OF MULTI-PHASES

As aforementioned, concrete can be treated as a composite with aggregate-, cement paste- and ITZ-phases. Compared with the cement paste and ITZs, aggregates are much denser and have much high

resistance to the transport of ions and therefore, in the present study they are assumed to be the impermeable material. The cement paste- and ITZ-phases can be treated as two individual porous materials with different transport properties. When applying the ionic transport equations from an electrolyte solution to a porous material, one has to consider the effects of porosity and tortuosity of the pore structure as well as the adsorption/desorption of ions at pore surfaces on the ionic transport in the porous material. The former is usually to be incorporated into the diffusion coefficient and the latter is often represented using ionic binding models. In this case, Eq. (2) need be modified as follows,

$$\frac{\partial(\varphi C_k)}{\partial t} + \frac{\partial[(1-\varphi)S_k]}{\partial t} = -\varphi \nabla \cdot \mathbf{J}_k \quad (5)$$

where  $\varphi$  is the porosity of the porous material and  $S_k$  is the concentration of bound ions. To eliminate  $\varphi$  and  $S_k$  in Eq. (5), the following Langmuir isotherm is often used to link the concentrations of bound and free ions,

$$\frac{(1-\varphi)S_k}{\varphi} = \frac{\alpha_k C_k}{w(1+\beta_k C_k)} \quad (6)$$

where  $w$  is the content of the water in which ionic transport takes place, expressed per unit weight of cement,  $\alpha_k$  and  $\beta_k$  are the constants which can be determined experimentally. Note that other chloride binding isotherms such as the linear and Freundlich isotherms could also be used, which will result in Eq. (6) to have different expressions. The use of Eqs. (1) and (6) in Eq. (5), yields,

$$(1+\lambda_k) \frac{\partial C_k}{\partial t} = \nabla \cdot (D_k \nabla C_k) + \nabla \cdot \left[ \left( \frac{z_k D_k F}{RT} \right) C_k \nabla \Phi \right] \quad (7)$$

where  $\lambda_k > 0$  is a dimensionless parameter for the  $k$ -th species defined as follows,

$$\lambda_k = \frac{\alpha_k}{w(1+\beta_k C_k)^2} \quad (8)$$

Eqs. (7) and (4) can be used to determine the electrostatic potential,  $\Phi$ , and the concentrations of individual ionic species,  $C_k$  ( $k=1,2,\dots,N$ ), at any point and any time in the domain of the porous material. Note that when Eqs. (4) and (7) are applied to the concrete material of aggregates, ITZs, and cement paste phases, one has to use different transport properties for aggregates, ITZs, and cement paste, whereas continuous conditions are imposed for ionic concentrations and ionic fluxes at the interfaces between different phases. The details of the geometric modelling of the concrete of multi-phases will be given in following section.

## 4.0 MODELING OF “DOUBLE MULTI”

The concretes modelled in previous studies [9-18] as well as the presented work are treated as a heterogeneous composite structure with three phases consisting of mortar matrix, coarse aggregates and ITZs. Fig.1 shows a series of the 2-D concrete numerical models with the same size of 50x50 mm and the volume fraction of  $V_{agg} = 0.5$ . In the figure the circular areas represent the impermeable aggregates with the radii ranging from 1.5 mm to 10 mm. Outside each aggregate, there is an aureole ITZ shell of tiny scale (40  $\mu$ m) wrapping the aggregate. Outside the ITZs, the remaining part of the concrete model represents the mortar matrix. The location of the aggregates was randomly generated using a MATLAB program.

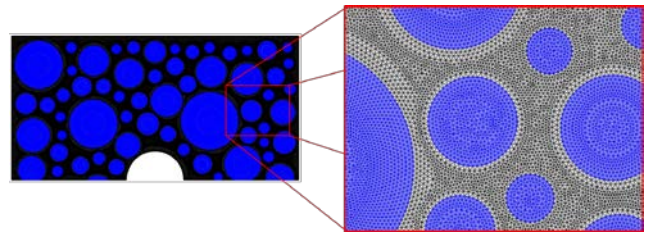


Fig. 1. Finite element mesh of the two phases concrete model ( $V_a=0.5$ )

The model described above is mainly used to simulate the ELM&ECR treatment of concrete. Fig. 2 graphically displays the simulated test, in which there are multi-component species governed by Eqs. (4) and (7). Due to the symmetry of the geometry of the specimen and the cathode settings, only a half of the specimen (50 mm x 25 mm) is modelled for simplifying calculation (as shown in Fig. 3). The initial and boundary conditions employed in the simulations are given in Table.1 [4].

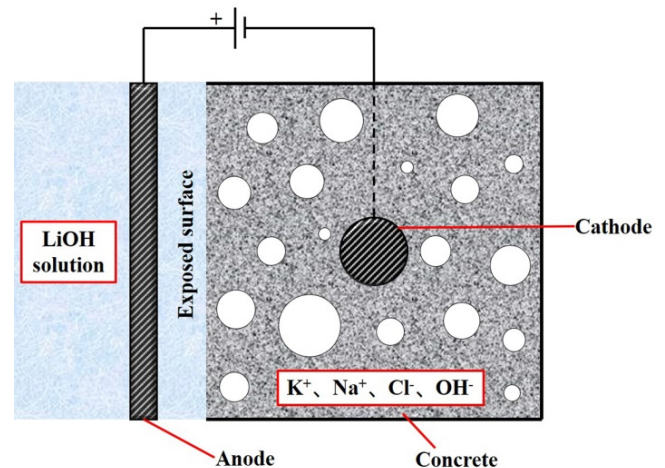
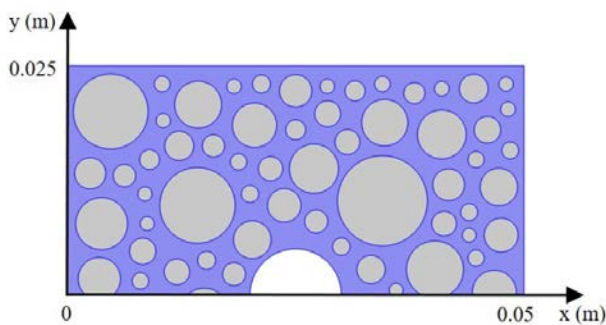


Fig. 2. Schematic representation of simulated ELM & ECR set up

**Table 1.** Information about five ionic species considered during modelling (25 °C)

Field variables	Potassium	Sodium	Chloride	Hydroxide	Lithium
Charge number	1	1	-1	-1	1
Diffusion coefficient in mortar phase, $\times 10^{-11}$ m <sup>2</sup> /s	3.900	2.700	10.20	52.80	3.700
Diffusion coefficient in aggregate phase, $\times 10^{-11}$ m <sup>2</sup> /s	0.039	0.027	0.102	0.528	0.037
Boundary concentration, mol/m <sup>3</sup> (at anode, $x=0$ )	5	5	10	1000	1000
Initial concentration in mortar phase, mol/m <sup>3</sup>	100	900	380	620	0

**Fig. 3.** The geometry of two phases mesoscale concrete model ( $V_a=0.5$ )

Assuming that the volume of the electrolyte reservoir at anode is much larger than that of the concrete sample, the concentration of lithium in electrolyte is assumed to be constant  $C_{Li0}$ .

By considering both the ionic electro-coupling interactions and heterogeneous nature of cement-based materials, the "multi-phase, multi-species" transport models for concrete, which is so-called "double multi" model, can be obtained

## 5.0 SIMULATION OF ELM & ECR

By using of the "double multi" model, one can solve a set of mechanism problems along the line of concrete durability study: ionic electro-coupling effect, diffusivity prediction, binding effect, EDL effect, cracking effect, ITZs, aggregate morphology, etc. This study shows a typical example of using this model, which is the simulation of ELM&ECR as mentioned.

The distribution contours of five ionic species ( $Cl^-$ ,  $K^+$ ,  $Na^+$ ,  $OH^-$ ,  $Li^+$ ) for specimens after 4-, 8- and 12-weeks treatment with a constant current density of  $2A/m^2$  are depicted in Figs. 4-8, respectively. In these 3-D plots,  $x$  and  $y$  coordinates show the change of the position in the model and the vertical coordinate represents the value of concentration. It

can be seen from these plots that the profiles of each species have its own unique characteristics.

Figure 4 shows a concave formed around the cathode for chloride under the external electric field. It can be observed that the chloride concentration gradually decreases from the initial value of  $380 \text{ mol/m}^3$  to only  $219 \text{ mol/m}^3$  (maximum value in concrete after 12-week treatment), which means ECR & ELM achieves a good performance of removing chlorides from concrete. Additionally, the chloride concentration near right boundary always reaches peak value, which demonstrates that the dominant process of ionic transport is still diffusion in the region out of the two electrodes, which makes the removal of chlorides harder. A closer observation also shows that there is a funnel-like pit around each aggregate since the great ionic diffusivity difference between aggregates and mortar

The positively charged potassium ions gradually gather around the rebar with time as shown in Fig. 5. The sodium ions also move towards rebar like potassium ions under the driving of the external current, therefore the distribution profiles of sodium are qualitatively similar with those of potassium as shown in Fig. 6. The peak values of sodium concentration are far greater than potassium, owing to its higher initial concentration in specimen. The accumulation of  $Na^+$  and  $K^+$  is of advantages for protecting rebar at cathode by locally increasing the pH and thus stabilizing the passive layer.

As shown in Fig. 7, the concentration around the cathode forms as convex for hydroxide ions, which is similar with the performances of two cations (i.e. potassium and sodium) rather than the negatively charged chlorides. This is because of that the electrochemical reactions taken place at the rebar surface provides an inward flux for the hydroxide ions. Notably, hydroxide ions concentration inside of whole concrete specimen gradually built up with the treatment time, which demonstrates that the hydroxide ions generated at the cathode are more than those move towards anode. Such behavior of hydroxides creates an alkaline environment in

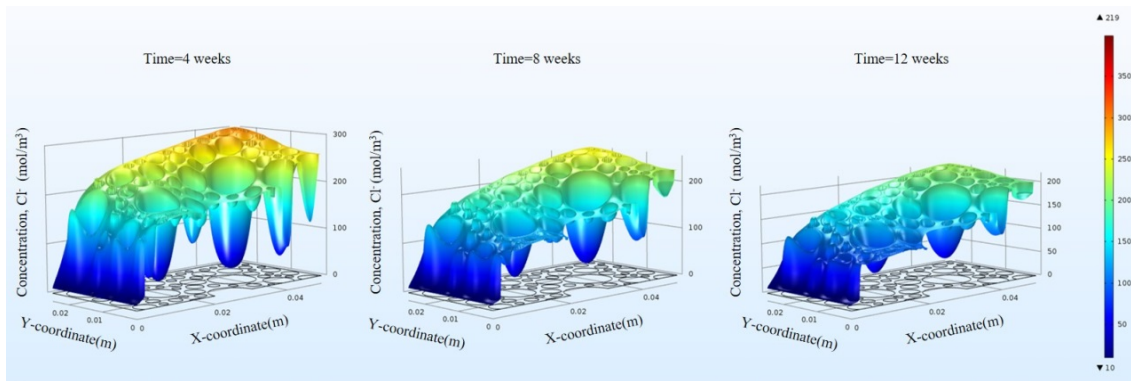


**Fig. 4.** Distribution profiles of chloride concentration at 4 weeks, 8 weeks and 12 weeks

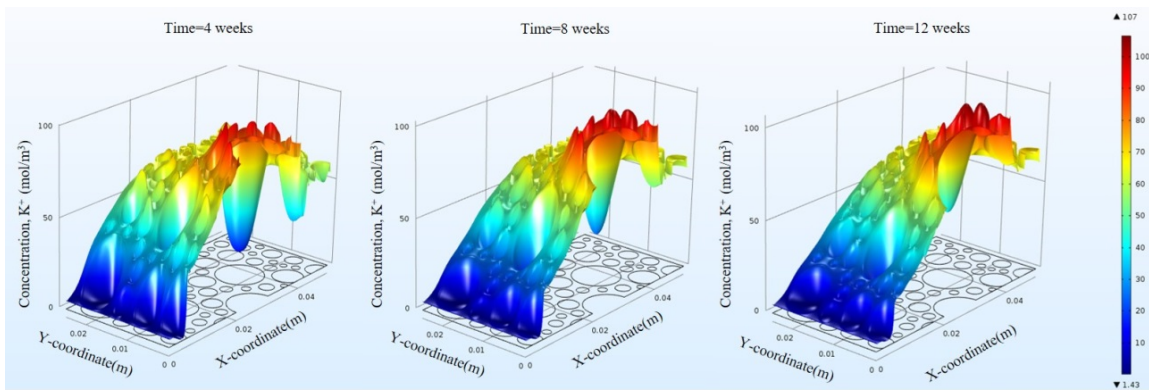


**Fig. 5.** Distribution profiles of potassium concentration at 4 weeks, 8 weeks and 12 weeks

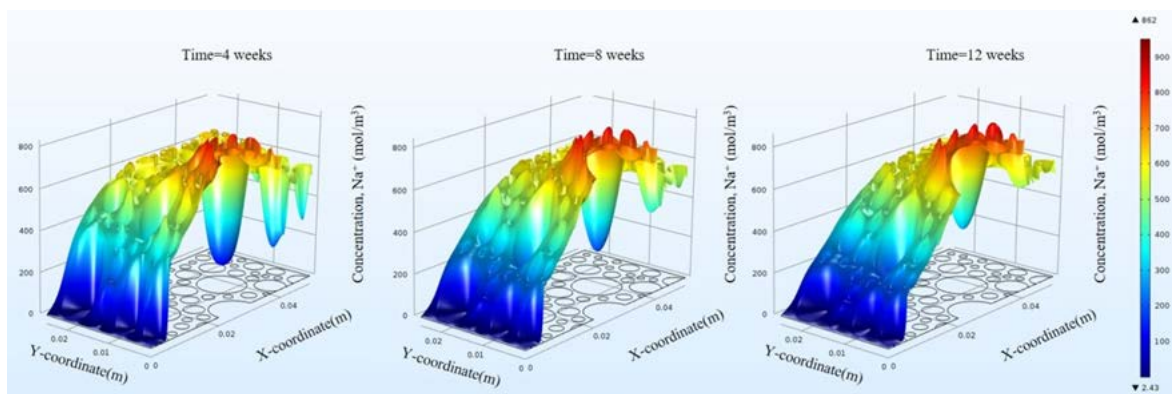


**Fig. 6.** Distribution profiles of sodium concentration at 4 weeks, 8 weeks and 12 weeks

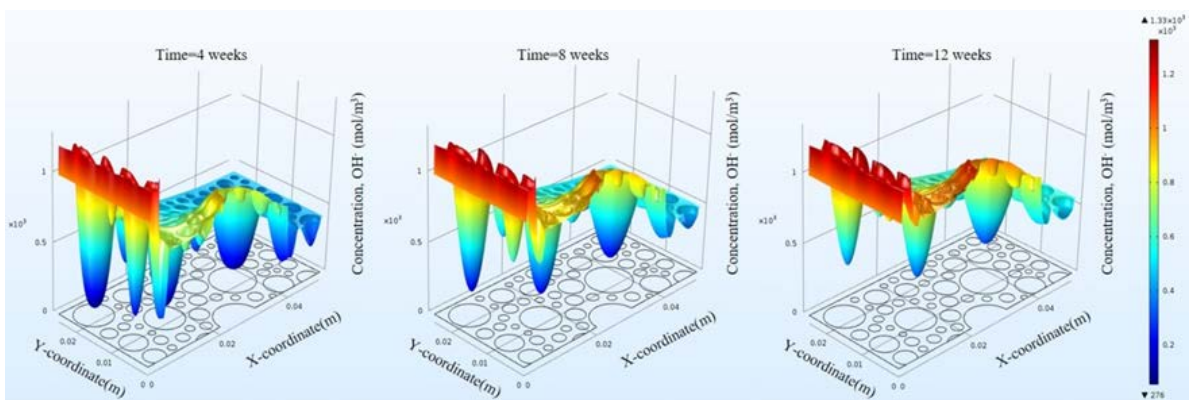


**Fig. 7.** Distribution profiles of hydroxide concentration at 4 weeks, 8 weeks and 12 weeks

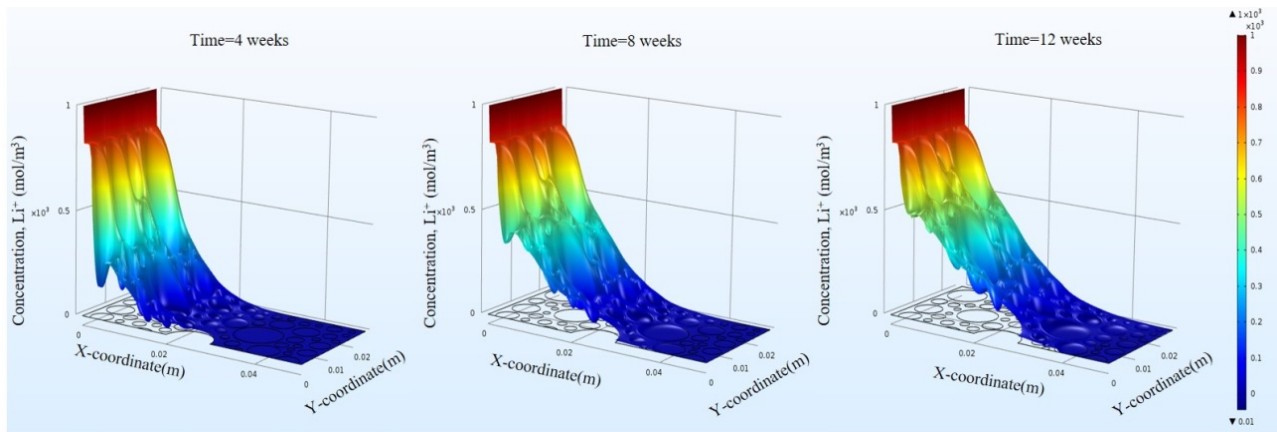


**Fig. 8.** Distribution profiles of lithium concentration at 4 weeks, 8 weeks and 12 weeks

specimen, which is beneficial to protect rebar from corrosion

It can be seen from the Fig. 8 that the contents and penetrations of lithiums in the specimen are built up with treatment time, which are meaningful to control ASR. It confirms that ECR and ELM is a very promising technique in driving lithiums into the concrete and reducing local chloride concentration in the vicinity of cathodes, which has been experimentally investigated by Ueda *et al.* (2013) and Buenfeld *et al.* (1998) and theoretically verified by Venglovska *et al.* (2016). From the contour plots, it can be noted that the lithium content is still very low behind the cathode after 12-week treatment, as limited current flow exists in this range, thereby the transport of lithiums driven by the electric field is much slower. The simulations of all ionic species agree well with the obtained shapes by Ueda *et al.* (2013, 2014) and exhibit the characteristics of each ionic species.

In order to further verify the reliability of the modelling, a simulated dummy test case is conducted by using the presented model with the parameters provide by Ueda's *et al* experiment (2014). The normalized lithium concentration in concrete ( $C_{Li}/C_{Li0}$ ) from numerical model after 8-week and the results from experiments are shown in Fig. 9, where  $C_{Li}$  is the lithium concentration in concrete and  $C_{Li0}$  is the concentration in electrolyte. It is clear that the numerical predictions agree well with the experimental data. The normalized lithium concentrations in concrete from modelling are higher than those of experiments in the range of 0-25mm depth. This is because of the assumption of constant concentration at boundaries during simulation based on partial differential equations (PDEs). However, it is apparent from the comparison that the tendency of the results from these two methods fits very well and most of the data points from the experiments after 8-week lie nearby or on the modelling results curve. The small fluctuation in the curve is mainly caused by the tortuosity variation due to the local distribution of aggregate particles.

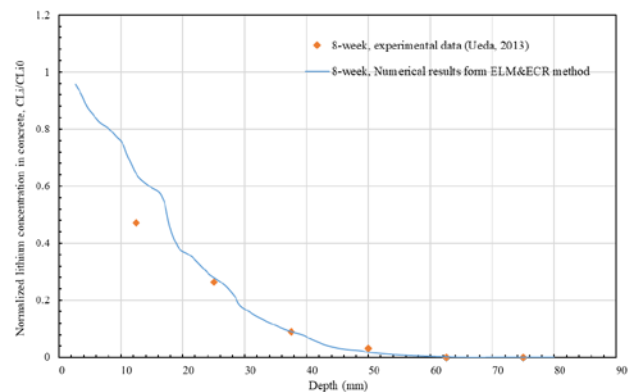


**Fig. 9** Comparisons of the lithium concentration in concrete obtained from ELM & ECR model and experimental data

## 6.0 CONCLUSIONS

The “double-multi” model, which was originally develop for a better understanding on ionic transport mechanisms in cement-based materials, is used to investigate the electromigration process of lithiums and chlorides in ASR affected concrete in the presented study. A special electrochemical treatment for driving lithium ions into concrete and removing chloride simultaneously was numerically investigated to mitigate the deterioration caused by ASR and chloride attack. The ionic interactions between different species, binding as well as the electrochemical reaction at electrodes are also considered. Based on the multi-phase and multi-species modeling, it was demonstrated that both the contents and penetration depth of lithium build up with treatment time. Sodium, potassium and hydroxide are found to be mainly located around or behind the rebar, while chloride has a low concentration around the rebar. Such performances of ions are beneficial to service life extension of reinforced concrete.

## Acknowledgement

The work was supported by the Natural Science Foundation of China (51508324), the Shanghai Chenguang Program, China (16CG06), and the Open Research Fund of State Key Laboratory of Simulation and Regulation of Water Cycle in River Basin, China Institute of Water Resources and Hydropower Research (IWHR-SKL-201705).

## References

- Bazant, Z. P. 1979. Physical model for steel corrosion in concrete sea structures—theory. *Journal of the Structural Division*, 105, 1155-1166.
- Buenfeld, N. R., Glass, G. K., HASSANEIN, A. M. & ZHANG, J.-Z. 1998. Chloride transport in concrete subjected to electric field. *Journal of Materials in Civil Engineering*, 10, 220-228.
- Geng, J., Easterbrook, D., Liu, Q. F. & Li, L. Y. 2016. Effect of carbonation on release of bound chlorides in chloride-contaminated concrete. *Magazine of Concrete Research*, 68, 353-363.
- Feng, G. L., LI, L. Y., KIM, B. & Liu, Q. F. 2016. Multiphase modelling of ionic transport in cementitious materials with surface charges. *Computational Materials Science*, 111, 339-349.
- Hu, Z., Mao, L. X., Xia, J., Liu, J. B., Gao, J., YANG, J. & LIU, Q. F. 2018. Five-phase modelling for effective diffusion coefficient of chlorides in recycled concrete. *Magazine of Concrete Research*, 70, 583-594.
- Li, L. Y. & Page, C. L. 2000. Finite element modelling of chloride removal from concrete by an electrochemical method. *Corrosion Science*, 42, 2145-2165.
- Liu, Q.-F., Easterbrook, D., Yang, J. & Li, L.-y. 2015a. A three-phase, multi-component ionic transport model for simulation of chloride penetration in concrete. *Engineering Structures*, 86, 122-133.
- Liu, Q.-F., Feng, G.-L., Xia, J., Yang, J. & Li, L.-Y. 2018. Ionic transport features in concrete composites containing various shaped aggregates: a numerical study. *Composite Structures*, 183, 371-380.
- Liu, Q.-F., LI, L.-Y., Easterbrook, D. & Yang, J. 2012. Multi-phase modelling of ionic transport in concrete when subjected to an externally applied electric field. *Engineering Structures*, 42, 201-213.
- Liu, Q.-F., XIA, J., Easterbrook, D., Yang, J. & Li, L.-Y. 2014. Three-phase modelling of electrochemical chloride removal from corroded steel-reinforced concrete. *Construction and Building Materials*, 70, 410-427.
- Liu, Q. F., Easterbrook, D., Li, L. Y. & Li, D. 2017b. Prediction of chloride diffusion coefficients using multi-phase models. *Magazine of Concrete Research*, 69, 134-144.
- Liu, Q. F., Yang, J., Xia, J., Easterbrook, D., Li, L. Y. & Lu, X. Y. 2015b. A numerical study on chloride migration in cracked concrete using multi-component ionic transport models. *Computational Materials Science*, 99, 396-416.
- Liu, Y. & Shi, X. 2012. Ionic transport in cementitious materials under an externally applied electric field: Finite element modeling. *Construction and Building Materials*, 27, 450-460.
- Martinez, I., Rozas, F., Ramos-Cillan, S., González, M. & Castellote, M. 2015. Chloride Electroremediation in reinforced structures: preliminary electrochemical tests to detect the steel repassivation during the treatment. *Electrochimica Acta*, 181, 288-300.
- Miyandehi, B. M., Feizbakhsh, A., Yazdi, M. A., LIU, Q. F., Yang, J. & Alipour, P. 2016. Performance and properties of mortar mixed with nano-CuO and rice husk ash. *Cement & Concrete Composites*, 74, 225-235.
- Page, C. & Yu, S. 1995. Potential effects of electrochemical desalination of concrete on alkali-silica reaction. *Magazine of concrete research*, 47, 23-31.
- Powers, T. & Steinour, H. An interpretation of some published researches on the alkali-aggregate reaction Part 1-The chemical reactions and mechanism of expansion. *Journal Proceedings*, 1955. 497-516.
- Rajabipour, F., Giannini, E., Dunant, C., Ideker, J. H. & THOMAS, M. D. A. 2015. Alkali-silica reaction: Current understanding of the reaction mechanisms and the knowledge gaps. *Cement and Concrete Research*, 76, 130-146.
- Ueda, T., Baba, Y. & Nanasawa, A. 2013. Penetration of lithium into ASR-affected concrete due to electro-osmosis of lithium carbonate solution. *Construction and Building Materials*, 39, 113-118.
- Ueda, T., Kushida, J., Tsukagoshi, M. & Nanasawa, A. 2014. Influence of temperature on electrochemical remedial measures and complex deterioration due to chloride attack and ASR. *Construction and Building Materials*, 67, 81-87.
- Venglovska, S., Pel, L. & Adan, O. C. G. 2016. Electromigration of lithium ions into cementitious materials as observed by NMR. *International RILEM Conference on Materials, Systems and Structures in Civil Engineering*.